ChemComm

COMMUNICATION

View Article Online
View Journal

Cite this: DOI: 10.1039/d6cc01485b

Received 11th March 2026,
Accepted 28th April 2026

DOI: 10.1039/d6cc01485b

rsc.li/chemcomm

Surfactant-free $NaBH_4$-mediated synthesis of Au_xPd_{1-x} nano-alloys for active electrocatalysts

Kristian Junker Andersen,[a] Armin Asghari Alamdari,[a] Aleksandra Smolska,[a] Nina Lock,[a] Anders Bentien[a] and Jonathan Quinson *[ba]

Nanomaterials with the composition Au_xPd_{1-x} (x = 0–1) in the size range of 5–15 nm are easily obtained at room temperature using a surfactant-free $NaBH_4$-mediated synthesis in water. These materials are readily active electrocatalysts suitable for the timely study of composition effects, as exemplified by the electrocatalytic ethanol oxidation reaction (EOR).

Nanomaterials (NMs) are relevant for a range of applications and in particular for catalysis due to their size-, structure-, and/or composition-dependent properties.[1] A range of methods have been reported to prepare such nanoparticles (NPs) with a large surface/volume ratio, especially relevant for catalysis.[2]

In particular, colloidal syntheses are tractable synthetic approaches, where typically a (metal) precursor in an oxidized state is reduced in the liquid phase.[1,3] Unfortunately, in most colloidal syntheses, additives or surfactants are used to ensure colloidal stability.[1,4] Those molecules typically bind to the NP surface, which prevents, in most cases, the full use of colloidal NPs for catalytic applications. Surfactant removal can be an option to address this challenge,[5] but it implies processes typically partially successful and/or requiring energy-intensive steps.[1]

To make the most of the versatility of colloidal syntheses[6] while by-passing the challenge of potentially blocked active sites, so-called surfactant-free colloidal syntheses are promising. Those syntheses are defined elsewhere and rely mainly on electrostatic stabilization.[1,7] In particular, surfactant-free colloidal syntheses carried out at room temperature in aqueous media using simple chemicals are attractive for safer operation, for potentially higher throughput and for providing a simple way to prepare NMs that is accessible to non-experts.[1,3,7,8]

Among reported options, Au NPs are easily obtained at room temperature in water without the need for any additives using solely $HAuCl_4$ as the precursor and $NaBH_4$ as the reducing agent.[9,10] A similar approach proved successful for the preparation of unsupported Pt,[11] Ru[12] and Pd[13] NMs, among other metals,[14] as detailed in the supplementary information (SI). The resulting NPs are promising candidates for catalysis (see Table S1).[9,11,12,15] For instance, surfactant-free Au NPs obtained by $NaBH_4$-mediated synthesis are readily active electrocatalysts for the ethanol oxidation reaction (EOR).[16] The EOR is relevant for energy conversion and is at the core of direct alcohol fuel cells.[17–19]

However, the use of this synthesis approach for the timely study of more complex compositions is seldom explored. To the best of our knowledge, only the synthesis of Au_xAg_{1-x} bimetallic NPs using this approach has been reported.[20] These NPs were used for 4-nitrophenol reduction as a model system for water treatment.

Here, we investigate whether bimetallic nanomaterials other than Au_xAg_{1-x} can be obtained to expand the generality and relevance of the synthesis approach. We use the fast and simple surfactant-free $NaBH_4$-mediated synthesis method to prepare Au_xPd_{1-x} NPs for electrocatalysis using the example of the EOR. It is well established that Pd is an efficient catalyst for the EOR with relatively poor stability and is prone to poisoning, whereas Au is less active but more stable.[8,21] The rationale for developing Au–Pd materials is also motivated here by the fact that Au[9,10] and Pd[13] monometallic NMs can be obtained using the proposed method. Au is expected to provide stability, whereas Pd exhibits activity for the EOR in alkaline media. In this sense, developing Au_xPd_{1-x} NPs is a promising and common strategy for the EOR[22,23] and other reactions.[24,25]

The first finding is that the surfactant-free $NaBH_4$-mediated synthesis yields NPs in seconds for the whole range of composition from Au only to Pd only, as illustrated in Fig. 1 and Fig. S1. In the present study, a total metal (Au + Pd) concentration of 0.5 mM and a $NaBH_4$/(Au + Pd) molar ratio of 5 were used. While the as-prepared Au colloids are stable for months, the stability decreases as the Pd content increases, in analogy to what was observed with Au_xAg_{1-x} with increasing amount of Ag,[20] and in agreement with the relatively lower stability of Pd colloidal materials prepared by the surfactant-free $NaBH_4$-mediated synthesis.[15]

[a] Biological and Chemical Engineering Department, Aarhus University, 40 Åbogade, 8200, Aarhus, Denmark
[b] CICA-Centro Interdisciplinar de Química e Bioloxía, Facultade de Ciencias, Universidade da Coruña, Campus de Elviña, A Coruña, Spain. E-mail: j.quinson@udc.es

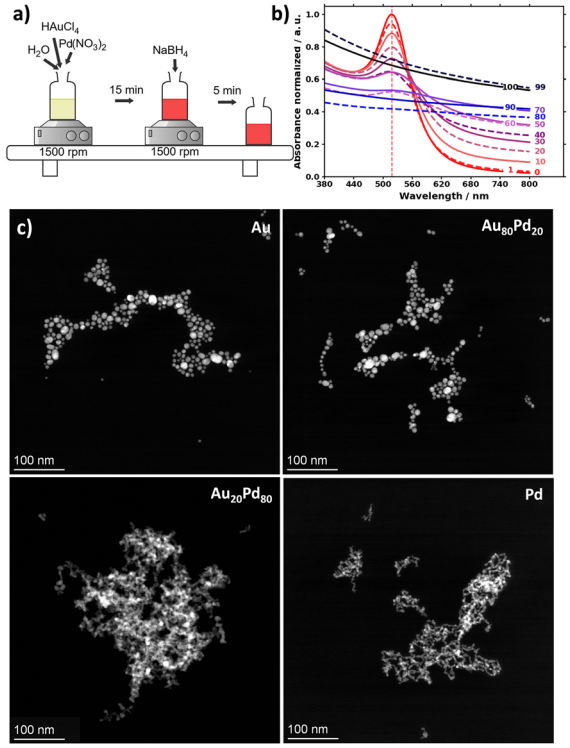

Fig. 1 (a) Schematic illustration of the room temperature $NaBH_4$-mediated surfactant-free synthesis of Au_xPd_{1-x} nanomaterials in water. Retrieved from https://chemix.org and adapted. (b) UV-vis characterization of the resulting materials; the nominal at% for Pd is indicated. (c) Illustrative STEM micrographs of samples prepared with Au (only), 20 at% Pd ($Au_{80}Pd_{20}$), 80 at% Pd ($Au_{20}Pd_{80}$), and Pd (only), as indicated.

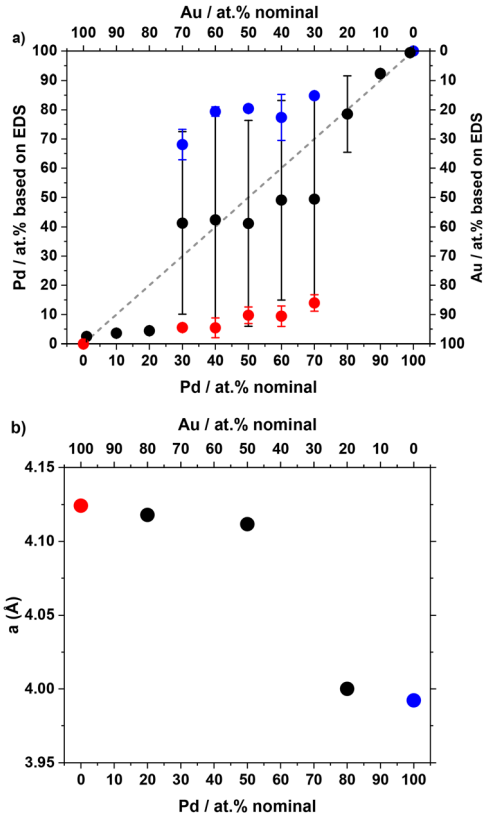

Fig. 2 (a) Experimental composition obtained from STEM–EDS as a function of nominal composition. For the samples showing two types of nanostructures, the composition obtained for the Au-rich population is indicated in red and that of Pd-rich nanomaterials is indicated in blue. (b) Lattice parameter as a function of nominal composition. See also Fig. S5.

Au-rich dispersions tend to exhibit red colour, whereas Pd-rich dispersions tend to be darker. The plasmonic properties assessed by UV-vis spectroscopy, marked by a pronounced surface plasmon resonance (spr) around 518 nm for Au NPs, become less pronounced as the Pd content increases, as can be expected[8] (see Fig. S2).

The size/shape of the NPs evaluated by STEM changes from a spherical to a network-like structure when the amount of Pd increases, which might account for the decreasing colloidal stability (see Fig. 1 and Fig. S3 and Table S2). The average size of the NMs is in the overall range of 5 to 15 nm.

UV-vis, STEM and EDS confirm that the composition and size can be tuned in the entire composition range by adjusting the ratio of the precursors (see Fig. 1c and 2). The discrepancy between nominal and experimental compositions obtained from EDS reported in Fig. 2a is commonly observed and attributed to experimental errors in the preparation of the stock solutions of metal precursors and/or quantification of the Au and Pd contents. Indeed, STEM–EDS considers only relatively few NPs. A mismatch between nominal and final compositions was also observed for Au_xPd_{1-x} materials prepared *via* a different route[8] and was also reported for Au_xAg_{1-x}.[20]

It is also interesting to note that the sample with a nominal Pd content from 30 at% up to 80 at% tends to show two populations of materials with some Au-rich and Pd-rich structures, as detailed in Fig. S4 and Fig. 2a. Within the same sample, the Au-rich structure tends to be spherical, whereas the Pd-rich structure tends to have a more network-like structure (see Fig. 1c). The Au-rich materials tend to be larger than the Pd-rich materials (see Fig. S3).

XRD analysis reveals a shift in diffraction patterns from the typical fcc structure of Au to the fcc structure of Pd with the change of the lattice parameter from *ca.* 4.12 Å (Au) to 4.00 Å (Pd) as the Pd content increases, as detailed in Fig. 2b and Fig. S5 and Table S2. The Au-rich NPs tend to be larger (see Fig. S3) and might dominate the volume-weighted XRD pattern, *e.g.* in the $Au_{50}Pd_{50}$ sample, which accounts for the trend observed in Fig. 2b.

Note that here there is no independent control over size, composition and shape at this stage. Independent control over these interlinked properties could be desirable to disentangle these effects in catalysis. In this direction, the $NaBH_4$/Au molar ratio was kept at 5 in the present study to minimize the amount of relatively harmful $NaBH_4$ used and because it was shown to lead to the smallest Au NPs in previous studies.[16,26] It is expected that increasing the $NaBH_4$/Au molar ratio and/or increasing the metal concentration or finer control over the pH will lead to larger NPs, by analogy with what was observed for Au and Au_xAg_{1-x} NPs in previous reports.[20,27]

The second finding is that the NPs are readily electrochemically active and can therefore be directly used to assess the EOR

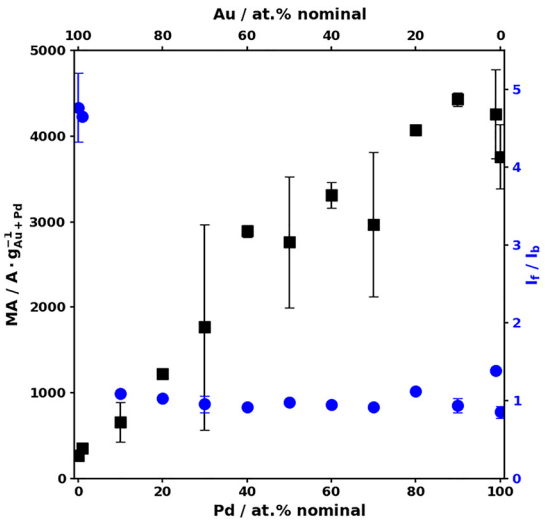

Fig. 3 MA (left-hand side *Y*-axis, black, ■) and I_f/I_b ratio (right-hand side *Y*-axis, blue, ●) as a function of the sample's nominal composition.

activity. Details on the typical data and metrics for this reaction are shown in the SI, Fig. S6–S11. The mass activity (MA, normalized to the nominal metal content) decreases as the Au content increases (see Fig. 3). The poisoning resistance tends to increase as the Au content increases, as observed with an overall increase of the I_f/I_b ratio, defined and detailed in the SI.[28]

The values obtained in terms of MA and poisoning resistance are promisingly high compared to the literature, in particular for Au–Pd materials,[19,28] as discussed further below.

It is expected that the nanocatalyst stability under electrochemical testing decreases with the Pd content, while the overpotential to observe catalytic behaviour decreases as the amount of Pd increases.[8] Given the potential benefits of Au NPs and Au-rich Au–Pd nanomaterials in terms of stability,[22,23] a more specific focus is here given to $Au_{50}Pd_{50}$ and $Au_{80}Pd_{20}$ as illustrative examples, compared to Au only, Pd only and $Au_{20}Pd_{80}$.

Chronoamperometry (CA) was performed at 0.9 V_{RHE} for Pd, $Au_{20}Pd_{80}$, $Au_{50}Pd_{50}$, and $Au_{80}Pd_{20}$, and at 1.2 V_{RHE} for Au, (see Fig. 4; see details in the SI and Fig. S11). The higher voltage needed for Au comes from the higher voltage at which catalysis is observed. The CA leads to a pronounced loss in MA as tabulated in Table 1. As the amount of Au decreases, the MA decreases, and hardly less than 1% of the original MA is maintained after 1 hour for the Pd-rich samples, whereas Au-rich samples retain up to 5–10% of their activity. Although the MA of the Pd-rich sample is expected to be higher as the Pd content increases (see Fig. 4), the relatively low current observed for the Pd-only sample illustrates the likely formation of oxidized Pd that is not catalytically active.[29] In particular, the $Au_{50}Pd_{50}$ sample shows initially high activity but a loss of MA of more than 99% for 1 hour of CA. In contrast, an Au-rich sample, such as $Au_{80}Pd_{20}$, shows a relatively low MA but maintains a relatively higher activity over time (loss of 95% based on CA).

After CA, performing several CVs reactivates the materials, as shown in Table 1 and Fig. S11. These results suggest that leaching is not the main mechanism of activity loss over time

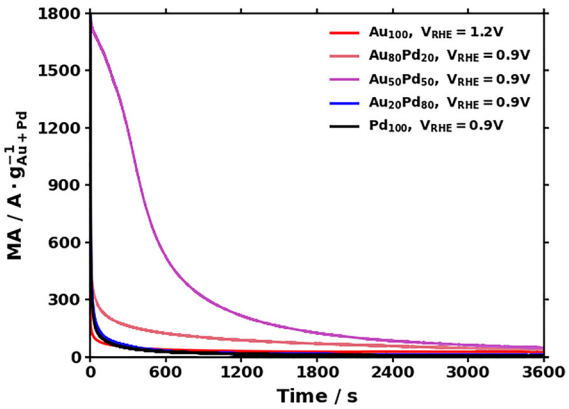

Fig. 4 CA in 1 M KOH + 1 M ethanol at 1.2 V_{RHE} for the Au sample and at 0.9 V_{RHE} for various other samples.

Table 1 MA maintained over time during CA performed for 1 hour at 0.9 V_{RHE}[a] in 1 M KOH with 1 M ethanol and before and after CA (assessed by CV)

Sample	MA maintained % (CA)[b]	MA maintained % (CV)[c]	No. of CV cycles before and after CA	V_{RHE} for CA
Au[a]	11.3	109.7	5	1.2
$Au_{80}Pd_{20}$	5.2	104.5	25	0.9
$Au_{50}Pd_{50}$	2.6	100.9	15	0.9
$Au_{20}Pd_{80}$	0.6	121.4	10	0.9
Pd	0.1	106.0	5	0.9

[a] CA performed for 1 hour at 1.2 V_{RHE} for the Au sample. [b] Compared to the activity recorded after 1 s of CA. [c] Based on CV before and after CA. The number of CVs before CA was chosen to reach a steady MA and the same number of CVs was performed after CA for comparison. The number of CVs is indicated in the fourth column.

and that further optimization of electrochemical testing could lead to higher catalytic activity maintained under continuous operation, *e.g.* by supporting the material.[3,30]

Finally, it is generally challenging to compare materials synthesized by different methods and with catalytic activity evaluated by different protocols in the literature (different syntheses, sizes, compositions, different setups, NPs supported or not on other materials, different concentrations and nature of electrolytes, different potential ranges, different normalization, *etc.*).[3,19,31,32] Nevertheless, the materials obtained here are relatively more active than those in other reports. The MA of 250 A g_{Au}^{-1} for Au NPs is higher than those reported in most other studies and comparable to values reported for Au NPs prepared by a surfactant-free ethanol-mediated synthesis reported elsewhere[28] and references therein. The MA of 4000 A g_{Pd}^{-1} for Pd NPs is higher than most reported values, which are closer to 3000 A g_{Pd}^{-1} or lower.[13,23,30,33] Similarly, bimetallic materials exhibit relatively high MAs (at similar compositions) compared to other Au–Pd materials in the range of 400–3000 A g_{Au+Pd}^{-1},[23,34] for instance, for materials obtained *via* a similar approach to the one reported here but with polyvinylpyrrolidone (PVP)[34] or Triton as additives.[35]

The results point towards the benefits of a surfactant-free approach leading to more active NPs and toward Au-rich

materials to develop promising catalysts for the EOR. Despite the relative inhomogeneity of the sample with Pd- and Au-rich materials within the same batch, the overall strategies still lead to active materials, probably due to further *in situ* alloying as reported elsewhere for nanocomposites;[8] however, a full study of such a phenomenon is beyond the scope of the present report.

On a final note, surfactant-free colloidal NPs remain relatively scarce compared to their surfactant-assisted counterparts, yet they are promising for developing catalysts.[1] As a consequence, the comparison of colloidal NPs obtained by different surfactant-free strategies is only emerging. In our previous work, we showed that Au_xPd_{1-x} NPs could be obtained at room temperature by simply using alkaline ethanol in water as the reducing agent.[8] The first benefit of using the milder reducing agent ethanol was that stable colloids were obtained for the entire range of composition from Au only to Pd only, as opposed to the present case. Furthermore, spherical NPs were obtained for the entire composition range. However, the synthesis is much slower than the present $NaBH_4$-mediated approach.

Interestingly, in that previous work,[8] an optimal composition of $Au_{65}Pd_{35}$ was identified to obtain higher MA for the EOR, in agreement with other work,[36] with a value around 2400 A $g_{Au+Pd}{}^{-1}$. This was attributed to a balance between the smaller size of Au_xPd_{1-x} NPs offering a higher surface area leading to a higher MA as the Pd amount increases, and the lower stability of the spherical small-sized Pd-rich NPs obtained. Here, no optimum is observed (see Fig. 3). This is attributed to a minor change in size (see Table S2), but a significant change in shape together with composition, where Pd-rich network like structures are likely more stable than small-sized spherical NPs for electrocatalysis; however, a detailed comparison is beyond the scope of this communication. Furthermore, the NPs obtained here for similar composition exhibit a higher MA of *ca.* 3000 A $g_{Au+Pd}{}^{-1}$, highlighting the potential benefits of surfactant-free $NaBH_4$-mediated synthesis for developing active catalysts.

The results highlight the under-tapped potential of surfactant-free room-temperature $NaBH_4$-mediated synthesis of multimetallic NPs in aqueous media as a simple strategy to obtain composition-controlled NMs directly relevant for electrocatalysis. The synthetic approach could be key to timely screening of larger parameter spaces for NP synthesis and/or catalysis and is relevant for addressing pending challenges in data-driven research.[37] Indeed, the synthesis enables a relatively high throughput due to its simplicity and short reaction time without the need for advanced facilities such as automated stations.

In conclusion, Au_xPd_{1-x} NPs with controlled overall composition are easily obtained at room temperature using a surfactant-free $NaBH_4$ mediated synthesis. The NPs are readily active materials for the EOR. The results show and stress the potential of this approach, probably under-exploited, to rapidly assess the effect(s) of composition on nano-alloys in (electro)catalysis.

Conceptualization: JQ; data curation: KJA, AAA, and AS; formal analysis: KJA, AAA, and AS; funding acquisition: JQ, NL, and AAA; investigation: KJA, AAA, and AS; methodology: JQ; project administration: JQ; resources: JQ and NL; supervision: JQ, NL, and AB; validation: KJA; visualization: KJA and AS; writing – original draft: JQ and KJA; writing – review & editing: KJA, AAA, AS, NL, AB, and JQ.

Conflicts of interest

There are no conflicts to declare.

Data availability

The data supporting this article have been included as part of the supplementary information (SI). Supplementary information: additional literature, materials and methods, characterization by XRD, STEM–EDS, UV-vis spectroscopy and electrochemical methods. See DOI: https://doi.org/10.1039/d6cc01485b.

Acknowledgements

J. Q., N. L. and A. S. thank the Independent Research Fund (DFF) for support *via* a DFF-Green grant (Light-SCREEN, 3164-00128B). The XRD instrument was supported by the Carlsberg Foundation (Grant no. CF18-0840). J. Q. thanks the Aarhus University Research Foundation (grant number AUFF-E-2022-9-40). J. Q. thanks the MCIN/AEI/10.13039/501100011033 and ESF+ for his Ramón y Cajal contract (RYC2023-042920-I). J. Q. thanks the INTALENT program of UDC and INDITEX. This work was funded by the European Union under the Marie Skłodowska-Curie Postdoctoral Fellowship (Project 101205473 – ZAIRWAYS, AAA). Views and opinions expressed are however those of the authors only and do not necessarily reflect those of the European Union or the European Research Executive Agency. Neither the European Union nor the granting authority can be held responsible for them. Funding for open access charge: Universidade da Coruña/CISUG.

References

1 J. Quinson, S. Kunz and M. Arenz, *ACS Catal.*, 2023, **13**, 4903–4937.
2 C. D. De Souza, B. R. Nogueira and M. Rostelato, *J. Alloys Compd.*, 2019, **798**, 714–740.
3 J. Quinson, S. Kunz and M. Arenz, *ChemCatChem*, 2021, **13**, 1692–1705.
4 L. M. Rossi, J. L. Fiorio, M. A. S. Garcia and C. P. Ferraz, *Dalton Trans.*, 2018, **47**, 5889–5915.
5 M. Cargnello, C. Chen, B. T. Diroll, V. V. T. Doan-Nguyen, R. J. Gorte and C. B. Murray, *J. Am. Chem. Soc.*, 2015, **137**, 6906–6911.
6 Y. T. Guntern, V. Okatenko, J. Pankhurst, S. B. Varandili, P. Iyengar, C. Koolen, D. Stoian, J. Vavra and R. Buonsanti, *ACS Catal.*, 2021, **11**, 1248–1295.
7 S. Reichenberger, G. Marzun, M. Muhler and S. Barcikowski, *ChemCatChem*, 2019, **11**, 4489–4518.
8 J. Quinson, O. Aalling-Frederiksen, W. L. Dacayan, J. D. Bjerregaard, K. D. Jensen, M. R. V. Jørgensen, I. Kantor, D. R. Sørensen, L. Theil Kuhn, M. S. Johnson, M. Escudero-Escribano, S. B. Simonsen and K. M. Ø. Jensen, *Chem. Mater.*, 2023, **35**, 2173–2190.
9 C. Deraedt, L. Salmon, S. Gatard, R. Ciganda, R. Hernandez, J. Ruiz and D. Astruc, *Chem. Commun.*, 2014, **50**, 14194–14196.
10 M. Iqbal, G. Usanase, K. Oulmi, F. Aberkane, T. Bendaikha, H. Fessi, N. Zine, G. Agusti, E. Errachid and A. Elaissari, *Mater. Res. Bull.*, 2016, **79**, 97–104.
11 R. P. Charde, B. van Devener and M. M. Nigra, *Catalysts*, 2023, **13**, 248.
12 S. Anantharaj, M. Jayachandran and S. Kundu, *Chem. Sci.*, 2016, **7**, 3188–3205.

13 A. Ipadeola, B. Salah, A. Ghanem, D. Ahmadaliev, M. Sharaf, A. Abdullah and K. Eid, *Heliyon*, 2023, **9**, e16890.
14 M. Wuithschick, S. Witte, F. Kettemann, K. Rademann and J. Polte, *Phys. Chem. Chem. Phys.*, 2015, **17**, 19895–19900.
15 F. Kettemann, M. Wuithschick, G. Caputo, R. Kraehnert, N. Pinna, K. Rademann and J. Polte, *CrystEngComm*, 2015, **17**, 1865–1870.
16 H. K. Fokam, A. Smolska and J. Quinson, *J. Mater. Chem. A*, 2026, DOI: 10.1039/D5TA08597G.
17 E. Antolini and E. R. Gonzalez, *J. Power Sources*, 2010, **195**, 3431–3450.
18 Y. Wang, S. Z. Zou and W. B. Cai, *Catalysts*, 2015, **5**, 1507–1534.
19 L. Yaqoob, T. Noor and N. Iqbal, *RSC Adv.*, 2021, **11**, 16768–16804.
20 N. E. Larm, J. A. Thon, Y. Vazmitsel, J. L. Atwood and G. A. Baker, *Nanoscale Adv.*, 2019, **1**, 4665–4668.
21 Y. Y. Feng, Z. H. Liu, Y. Xu, P. Wang, W. H. Wang and D. S. Kong, *J. Power Sources*, 2013, **232**, 99–105.
22 L. S. R. Silva, C. V. S. Almeida, C. T. Meneses, E. A. Batista, S. F. Santos, K. I. B. Eguiluz and G. R. Salazar-Banda, *Appl. Catal., B*, 2019, **251**, 313–325.
23 B. Hanqi, J. Xu, X. Zhu and C. Kan, *Nanoscale Adv.*, 2022, **4**, 1827–1834.
24 Y. Zhang, Z. Lyu, Z. Chen, S. Zhu, Y. Shi, R. Chen, M. Xie, Y. Yao, M. Chi, M. Shao and Y. Xia, *Angew. Chem., Int. Ed.*, 2021, **60**, 19643–19647.
25 X. Y. Huang, O. Akdim, M. Douthwaite, K. Wang, L. Zhao, R. J. Lewis, S. Pattisson, I. T. Daniel, P. J. Miedziak, G. Shaw, D. J. Morgan, S. M. Althahban, T. E. Davies, Q. He, F. Wang, J. L. Fu, D. Bethell, S. McIntosh, C. J. Kiely and G. J. Hutchings, *Nature*, 2022, **603**, 271–275.
26 K. J. Andersen, M. Varga, A. Smolska, G. Nordhal, J. H. Jensen, R. Moreno, E. D. Bøjesen, A. S. Anker and J. Quinson, *Nano Lett.*, 2025, **25**, 15436–15442.
27 J. Quinson, A. Dworzak, S. B. Simonsen, L. T. Kuhn, K. M. O. Jensen, A. Zana, M. Oezaslan, J. J. K. Kirkensgaard and M. Arenz, *Appl. Surf. Sci.*, 2021, **549**, 149263.
28 D. Panagopoulos, A. Asghari Alamdari and J. Quinson, *Mater. Today Nano*, 2025, **29**, 100600.
29 Z. Liang, T. Zhao, J. Xu and L. Zhu, *Electrochim. Acta*, 2009, **54**, 2203–2208.
30 J. Quinson, S. B. Simonsen, L. T. Kuhn, S. Kunz and M. Arenz, *RSC Adv.*, 2018, **8**, 33794–33797.
31 A. R. Zeradjanin, *ChemSusChem*, 2018, **11**, 1278–1284.
32 S. Nösberger, J. Du, J. Quinson, E. Berner, A. Zana, G. K. H. Wiberg and M. Arenz, *Electrochem. Sci. Adv.*, 2022, **3**, e2100190.
33 L. Zang, J. Yan, M. Pang, B. Zhang, J. Chen and P. Guo, *Langmuir*, 2021, **37**, 13132–13140.
34 S. Y. Shen, Y. G. Guo, L. X. Luo, F. Li, L. Li, G. H. Wei, J. W. Yin, C. C. Ke and J. L. Zhang, *J. Phys. Chem. C*, 2018, **122**, 1604–1611.
35 L. Wang, Z. Liu, S. Zhang, M. Li, Y. Zhang, Z. Li and Z. Tang, *Int. J. Hydrogen Energy*, 2021, **46**, 8549–8556.
36 H. H. Lin, M. Muzzio, K. C. Wei, P. Zhang, J. R. Li, N. Li, Z. Y. Yin, D. Su and S. H. Sun, *ACS Appl. Energy Mater.*, 2019, **2**, 8701–8706.
37 R. W. Epps and M. Abolhasani, *Appl. Phys. Rev.*, 2021, **8**, 041316.